Histol Histopathol (2021) 36: 305-315

http://www.hh.um.es

Histology and Histopathology
From Cell Biology to Tissue Engineering

ORIGINAL ARTICLE **Open Access**

Frequent *DYRK2* gene amplification in micropapillary element of lung adenocarcinoma - an implication in progression in *EGFR*-mutated lung adenocarcinoma

Chihiro Koike[1], Koji Okudela[1], Mai Matsumura[1], Hideaki Mitsui[1], Takehisa Suzuki[1], Hiromasa Arai[2], Toshiaki Kataoka[1], Yoshihiro Ishikawa[3], Shigeaki Umeda[1], Yoko Tateishi[1] and Kenichi Ohashi[1]

[1]Department of Pathology, Yokohama City University, School of Medicine, [2]Division of General Thoracic Surgery, Kanagawa Prefectural Cardiovascular and Respiratory Center Hospital and [3]Department of General Thoracic Surgery, Yokohama City University, School of Medicine, Yokohama, Japan

Summary. The present study aimed to discern the molecular alterations involved in the progression of *EGFR*-mutated lung adenocarcinoma (LADC). We previously demonstrated that the micropapillary (mPAP) element is the most important histological factor for assessing malignant grades in LADCs. Therefore, mPAP and other elements were separately collected from three cases of *EGFR*-mutated LADC using laser capture microdissection and subjected to a comprehensive mRNA expression analysis. We focused on DYRK2 in this study because its level showed a substantial increase in *EGFR*-mutated LADCs with mPAP. We also immunohistochemically examined 130 tumors for the expression of DYRK2. The results confirmed a strong expression of DYRK2 in *EGFR*-mutated LADC with mPAP. Fluorescent *in situ* hybridization (FISH) analyses targeting the DYRK2 locus revealed frequent gene amplification in *EGFR*-mutated LADC, specifically occurring in the high-grade components, like mPAP. In summary, the results of this study suggest that DYRK2 overexpression through gene amplification is one of the molecular mechanisms responsible for promoting the progression of *EGFR*-mutated LADC.

Key words: DYRK2, Lung adenocarcinoma, *EGFR* mutations, Micropapillary, Adenocarcinoma progression

Corresponding Author: Koji Okudela, Department of Pathology, Yokohama City University Graduate School of Medicine, 3-9, Fukuura, Kanazawa-ku, 236-0004, Yokohama, Japan. e-mail: kojixok@yokohama-cu.ac.jp

DOI: 10.14670/HH-18-294

Introduction

Lung cancer is a leading cause of cancer-related deaths worldwide, and lung adenocarcinoma (LADC) is the most common histological type. Numerous driver oncogenes, such as *EGFR, KRAS, ALK, RET,* and *ROS*, have been identified to date, most of which have been specifically targeted for drugs used in clinical practice (Paez et al., 2004; Soda et al., 2007; Ou, 2011; Takeuchi et al., 2012; Gainor and Shaw, 2013; Gainor et al., 2013). Therefore, LADCs are now classified based on driver mutations.

EGFR is the most common driver oncogene in LADCs and has several unique features. *EGFR*-mutated LADC occurs in non-smokers and females and has the histological feature of a lepidic element (Kosaka et al., 2004; Okudela et al., 2010; Villa et al., 2014). Although its features are generally associated with a favorable outcome (Warth et al., 2012; Kadota et al., 2014), some patients with *EGFR*-mutated LADC still show a rapid progression to death. We recently demonstrated that the highly malignant activity of *EGFR*-mutated LADC could be determined based on the mPAP element (Matsumura et al., 2016). mPAP has an unstable structure without a scaffold, unlike papillary growth with a conventional vascular axis. This histological feature is known to be associated with high aggressiveness (lymphatic canal invasion and lymph node metastases) in adenocarcinomas of different organs including the urinary bladder and mammary gland. Molecular alterations associated with mPAP have also been reported. For example, downregulation of miR-296 and activation of the RUVBL1 has been reported in bladder cancer (Guo et al., 2016). In colorectal cancer, survivin expression is reduced (Patankar et al., 2018). In breast cancer, BC-1514 expression is upregulated in mPAP

(Kanomata et al., 2019). In lung cancer, overexpression of cMET has been reported (Zhang et al., 2018). However, the underlying molecular causes and mechanisms to explain the relationship between the distinctive morphology and high malignant activity of mPAPs remain unclear.

Herein, we attempted to elucidate the molecular mechanisms producing the mPAP element in *EGFR*-mutated LADC through comprehensive mRNA expression analysis.

Materials and methods

Patients

Patients with LADC who underwent surgical lung resection at the Kanagawa Prefectural Cardiovascular and Respiratory Center (Yokohama, Japan) and Yokohama City University Hospital (Yokohama, Japan) between May 2002 and December 2018 were examined. Written informed consent was obtained for the use of these samples for research purposes. The Ethics Committees of the Kanagawa Prefectural Cardiovascular and Respiratory Center Hospital and Yokohama City University Hospital approved our research plan.

Histopathological examination

Tissue sections were cut from formalin-fixed paraffin-embedded tumor tissues then stained with hematoxylin and eosin (HE). The proportions of the histological subtypes (lepidic, acinar, papillary, mPAP, solid elements, and variants) were described in 5% increments according to the World Health Organization classification system (Travis et al., 2015). Two pathologists (C.K. and K.O.) reviewed all the HE-stained tissue sections and reached a consensus on histological element proportions.

Immunohistochemistry

Tumor tissues were fixed with buffered 10% formaldehyde solution and embedded in paraffin wax. Sections were deparaffinized, rehydrated, and incubated with blocking solution, inhibiting endogenous peroxidase activities and non-immunospecific protein binding. The sections were boiled in Tris buffer (0.01 M, pH 9.0) to retrieve the masked epitopes then incubated with primary antibodies against DYRK2 (Abgent, San Diego, CA), p53 (DO-7, DAKO, Carpinteria, CA), and Ki-67 (SP6, Abcam, London, UK). Immunoreactivity was visualized using an Envision Detection System (DAKO), and nuclei were counterstained with hematoxylin.

The intensity of the DYRK2 immunohistochemical signal in the neoplastic cells was judged as negative (intensity 0), weak (intensity 1), or strong (intensity 2). The DYRK2 scores were calculated as follows: [score=1×(proportion of the area with weak intensity) + 2×(proportion of the area with strong intensity)]. The Ki-67 labeling index was calculated by counting 200-500 tumor cells in the desired areas. *p53* expression was judged as "positive" when nuclei showing unequivocally strong signals were diffusely present. Two pathologists (C.K. and K.O.) reached a consensus on the results of immunohistochemistry for DYRK2 and p53.

Mutational analysis of the EGFR gene

EGFR mutations (exons 18, 19, 20, and 21) in surgically resected tumors were analyzed by direct DNA sequencing, as described previously (Lynch et al., 2004; Okudela et al., 2009). The Scorpion amplification refractory mutation system was used to search for mutations in small biopsy samples (Kimura et al., 2006; Goto et al., 2012).

Gene-chip microarray analysis

Total RNA was extracted using an RNeasy® Micro Kit (Qiagen, Venlo, Netherlands). We outsourced the experiments using the Gene-Chip Human Genome U133 Plus 2.0 Array (Affymetrix®, Santa Clara, CA) to TAKARA BIO INC. The results were provided as CEL file format (supplementary materials). We narrowed the differentially expressed genes using free computer software "Glis" (TAKARA). We examined six samples (two samples from each of three tumors). Microarray analysis was performed once per sample. The raw data are available in supplemental materials.

Quantitative reverse-transcription PCR (qRT-PCR)

We chose 54 tumors whose RNA stock condition was sufficient for quantitative analysis, and we examined the mRNA levels for DYRK2 (NM_006482), KIAA1324 (NM_020775), COL4A3 (NM_000091), ITGBL1 (NM_004791), and GAPDH (NM_0012 56799.3). Total RNA was extracted using the RNeasy Kit (Qiagen). First-strand cDNA was synthesized using the SuperScript First-Strand Synthesis System according to the manufacturer's instructions (Invitrogen, Carlsbad, CA). Quantitative reverse-transcriptase PCR using SYBR Premix EXTaq (Takara, Tokyo, Japan) was run in quadruplicate for each sample (n=54) on a Thermal Cycler DICE real-time PCR system (Takara). The primer sets used were as follows: forward (F) 5' - CAAGG CCTACGATCACAAAGT and reverse (R) 5' - AAATT CTCCAGCATATGGATGA for DYRK2, F 5' - ACAACAAGATCCACTCTCTGTGCTA and R 5' - GACTGAGGGTAAAGTGATGGAAGTA for KIAA1 324, F 5' - CCAGGTCTCAAAGGATTCGC and R 5' - ATTCCCAGTGCTGCCCAAAT for COL4A3, F 5' - GGCAAATGCACCTGCTATCC and R 5' - TCACA AACACAGCGACCACA for ITGBL1, F 5' - GGTCG TATTGGGCGCCTGGT and R 5' - TACTCAGCG CCAGCATCGCC for GAPDH. Two similar mRNA expression values were used to calculate a mean value

for each gene. Expression levels were normalized to GAPDH levels.

Fluorescent in situ hybridization (FISH) for DYRK2

To assess the status of the DYRK2 gene locus, FISH analyses were performed on formalin-fixed paraffin-embedded sections. The probes used were RP11-92J17 (for the DYRK2 locus) and RP11-152M7 (for the locus near the centromere of chromosome 12). These clones were purchased from Advanced GenoTechs Co. (Tsukuba City, Japan). The probes were labeled with SpectrumGreen™ and SpectrumOrange™ using a labeling kit (Enzo Life Sciences, Farmingdale, NY). The tissue sections were incubated in a pre-treatment solution at 98°C for 15 min and then incubated with pepsin solution at 37°C for 15 min to digest the proteins. The sections were then hybridized with the probes (82°C for 5 min followed by incubation at 37°C overnight). After washing with wash buffer solution at 50°C for 10 min, the sections were mounted with DAPI. The number of dot signals was counted in 50 nuclei. A signal ratio of DYRK2/centromere (FISH score) of >2 was adjudged as amplification.

Statistical analysis

The relationship between the immunohistochemical (or FISH) scores and histological subtypes was analyzed using the Mann-Whitney U and Wilcoxon signed-rank tests. $P<0.05$ was considered significant. All analyses were performed using JMP 9.0.2 (SAS Institute, Cary, NC).

Results

Differentially expressed genes in the mPAP element

The mPAP and other elements were separately collected from the frozen tissue sections of three *EGFR*-mutated LADC cases using laser capture microdissection (Fig. 1). Samples were subjected to comprehensive mRNA expression analysis. Differentially expressed genes showing more than 3-fold change in the mPAP element compared to the other elements were selected (Tables 1, 2). The results are summarized in Figure 2. The expression levels of KIAA1324 (NM 020775) and DYRK2 (NM 006482) were found to be upregulated in all three cases, while those of COL4A3 (NM 000091) and ITGBL1 (NM 004791) were downregulated (Fig. 2).

Validation of the mRNA levels of the four selected genes

The levels of DYRK2, KIAA1324, COL4A3, and ITGBL1 were examined using qRT-PCR. Case 3 mRNA levels were not analyzed due to insufficient RNA following gene-chip analysis. DYRK2 and KIAA1324 levels were higher (the change in the levels of DYRK2

Table 1. Up-regulated genes.

Gene	Accession	Signal ratio		
		Case 1	Case 2	Case 3
KIAA1324	NM 020775	3.25	2.31	2.65
DYRK2	NM 006482	2.22	1.92	2.02
S100A9	NM 002965	5.69	2.1	0.03
CEACAM7	NM 006890	3.2	2.6	0.15
MMP12	NM 002426	3.26	3.84	1.45
TMEM150C	BF508344	2.54	5.1	1.04
TRIM68	NM 018073	3	2.05	0.34
LRMP	NM 006152	2.77	2.81	-1.24
EPHX1	NM 000120	2.43	1.6	-0.21
TNFRSF21	NM 016629	1.91	2.51	1.02
TTC9	BE675549	1.94	1.92	0.2
SGPP2	AW779536	1.9	2.08	0.39
DTWD2	H29590	1.76	1.82	0.34
SLITRK6	AI680986	2.22	0.83	1.79
CAND1	NM 018448	2.16	0.69	2
SRPX2	NM 014467	1.65	-0.1	1.76
PCDH20	AA040057	1.87	0.75	1.93
TBC1D30	AW134976	2.81	-0.62	2.15
DHCR24	NM 014762	1.7	-0.21	2.07
CNOT2	AL137674	1.65	0.08	1.73
HIST1H2AC	AL353759	1.64	1.14	1.86
ELOVL6	NM 024090	0.25	3.07	2.4
AURKA	NM 003158	-0.54	2.89	1.79
TOP2A	AU159942	-0.48	2.87	1.8
PGC	NM 002630	0.51	2.51	1.59
SLC35E3	NM 018656	0.34	2.43	2.73
KCNJ2	AF153820	0.59	2.13	1.97
FAM111B	AA960844	1.02	1.94	1.89
METTL14	AA573115	0.7	1.92	1.93
MAGED1	AF217963	0.72	1.83	1.7
CPNE4	AI703256	0.15	1.69	1.97

Gene, common gene name; accession, the GenBank accession number; signal ratio, log2 ratio of the micropapillary element to those of the other elements.

Table 2. Down-regulated genes.

Gene	Accession	Signal ratio		
		Case 1	Case 2	Case 3
COL4A3	NM 000091	-3.76	-2.01	-1.97
ITGBL1	NM 004791	-1.81	-1.68	-2.01
CYR61	NM 001554	-2.89	-4.82	-0.45
ESYT3	AI697584	-2.82	-1.89	-0.72
WIF1	NM 007191	-2.69	-4.66	-0.48
DUSP1	NH 004417	-1.72	-1.94	2.15
PLXDC2	AI278204	-1.68	-1.82	-0.45
ABCC9	NH 020297	-2.13	-0.22	-1.79
SHISA3	AI735586	-2.33	-2.88	-2.51
FGF14	AF339819	-4.24	-1.42	-2.09
FGFR3	NM 000142	-2.76	-0.92	-1.68
AHNAK2	BC004283	-2.48	-1.87	-1.64
MTSS1	NM 014751	-1.68	-0.51	-1.9
CST1	NM 001898	-1.69	-0.95	-1.93

Gene, common gene name; accession, the GenBank accession number; signal ratio, log2 ratio of the micropapillary element to those of the other elements.

in case 3 expression seemed slight), while those of COL4A3 and ITGBL1 were lower with the mPAP element (Fig. 3), consistent with the results obtained from the U133 gene-chip microarray analysis. Fifty-four additional LADC samples were examined. Similar results were obtained, but statistically significant differences were not found between tumors with and without the mPAP element (Fig. 4). Here, we focused on DYRK2, particularly because of its biological functions, such as the regulation of cell growth and apoptosis (Taira et al., 2007; Nihira and Yoshida, 2015).

Immunohistochemical analysis of DYRK2 expression

As described above, the difference in DYRK2 mRNA levels was not significant. This may be attributed to the small proportion of mPAP element in the tumor that was insufficient to produce a significant difference in analyses when using the bulk of the tumors. Therefore, we immunohistochemically examined 130 LADC samples (Table 3) for the expression of *DYRK2* in the largest tumor sections to analyze its level, specifically in the different histological elements. The results revealed that the mPAP element strongly expressed DYRK2. Representative images of LADC with different immunohistochemical levels of DYRK2 are shown in Figure 5. The expression levels were semi-quantified using the scoring system described above. *EGFR*-mutated LADC with the mPAP element consistently showed significantly higher DYRK2 scores than the other elements (Mann-Whitney U test, P = 0.0458, Fig. 6). While among the LADCs without *EGFR* mutations, the tumors with the mPAP element showed higher DYRK2 scores than those without the mPAP

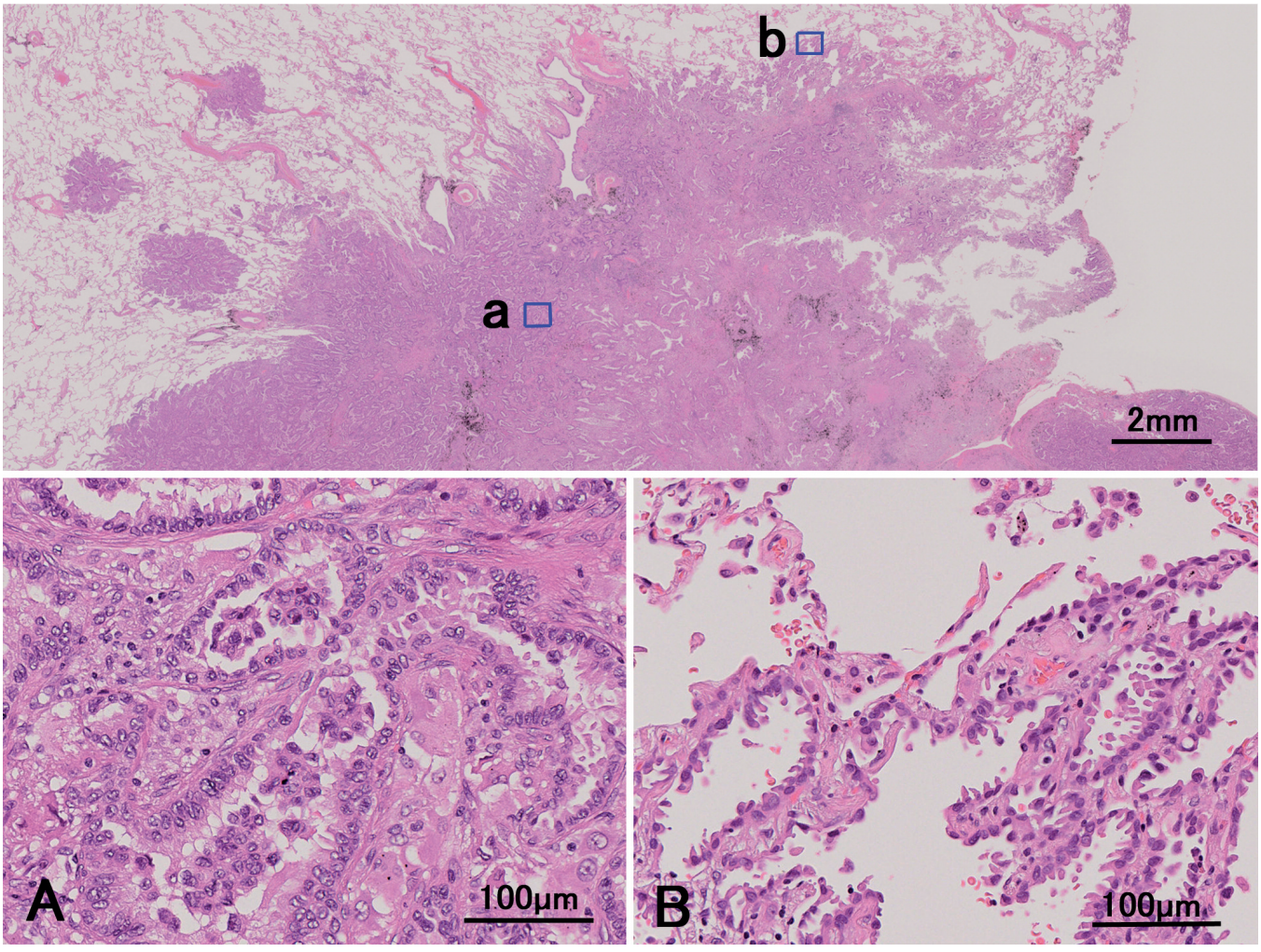

Fig. 1. Representative image of a tumor (hematoxylin and eosin-stained) subjected to laser capture microdissection. In the scanning view, the close-up view of the square 'a' represents the high-grade component **(A)** and the close-up view of square 'b' represents the low-grade component **(B)**. The high-grade component includes micropapillary and low papillary elements, and the low-grade consists of lepidic elements. Scale bars: scanning view, 2 mm; A and B, 100 μm.

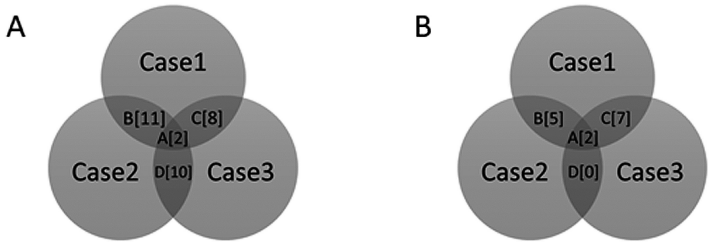

A: KIAA1324, DYRK2

B: S100A9, CEACAM7, MMP12, TMEM150C, TRIM68, LRMP, EPHX1, TNFRSF21, TTC9, SGPP2, DTWD2,

C: SLITRK6, CAND1, SRPX2, PCDH20, TBC1D30, DHCR24, CNOT2, HIST1H2AC

D: ELOVL6, AURKA, TOP2A, PGC, SLC35E3, KCNJ2, FAM111B, METTL14, MAGED1, CPNE4

A: COL4A3, ITGBL1

B: CYR61, ESYT3, WIF1, DUSP1, PLXDC2

C: ABCC9, SHISA3, FGF14, FGFR3, AHNAK2, MTSS1, CST1

D: Nothing

Fig. 2. Venn diagrams based on the results from the three gene-chip microarray analyses. Upregulated genes **(A)** and downregulated genes **(B)** with more than 3-fold changes in the high-grade component compared to the low-grade component were selected.

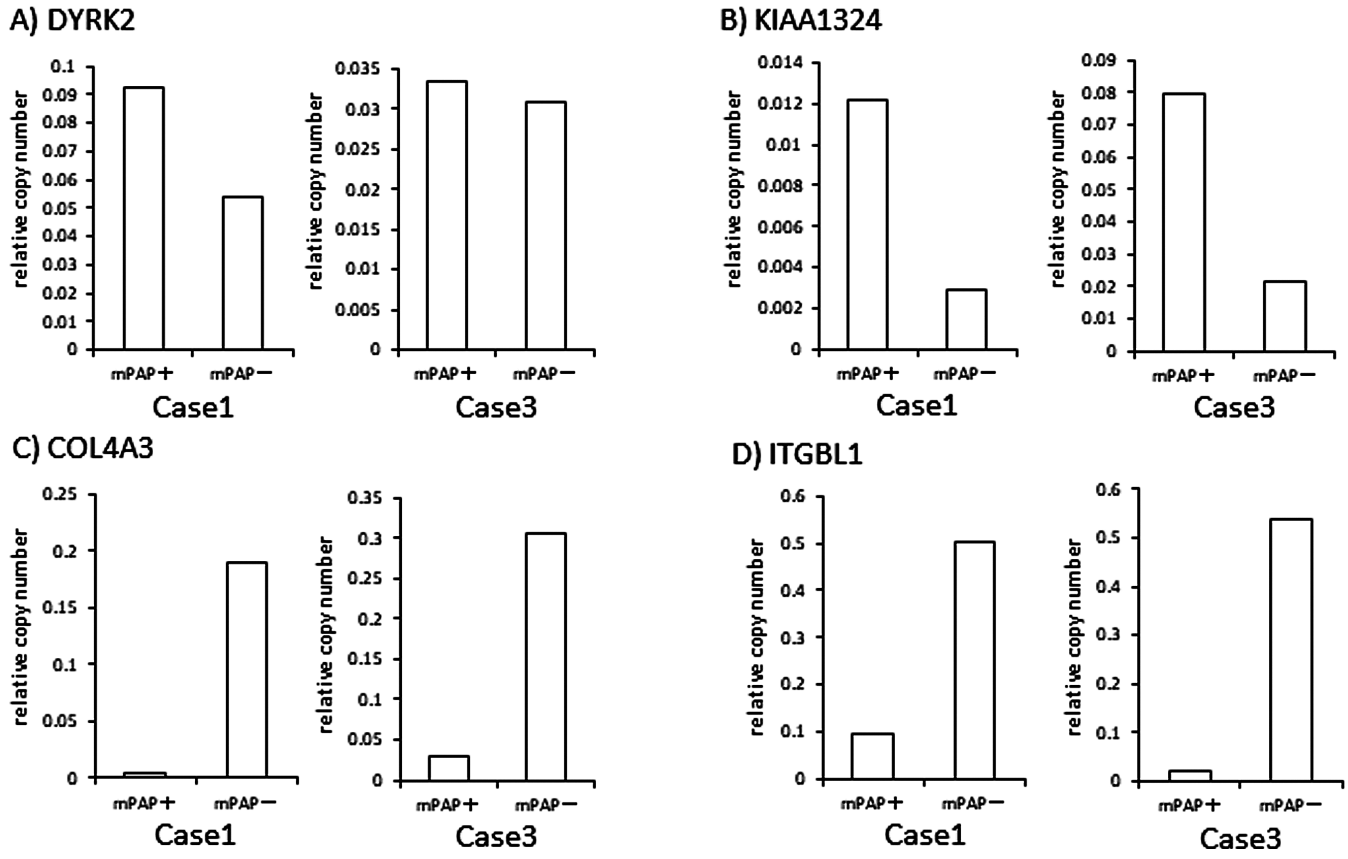

Fig. 3. mRNA levels of DYRK2 **(A)**, KIAA1324 **(B)**, COL4A3 **(C)**, and ITGBL1 **(D)** in two *EGFR*-mutated LADC cases subjected to gene-chip microarray analyses. Relative copy numbers normalized to GAPDH are plotted. mPAP+, high-grade component including the mPAP element; mPAP-, low-grade component of the lepidic element.

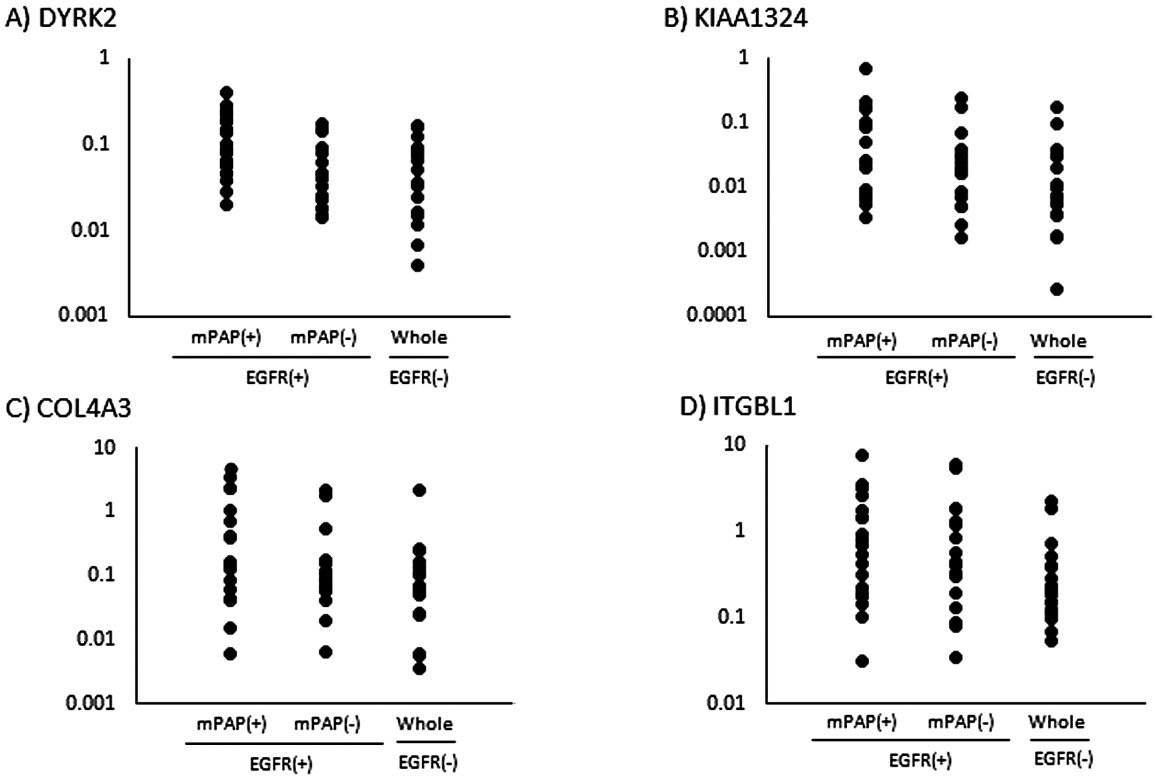

Fig. 4. mRNA levels of DYRK2 **(A)**, KIAA1324 **(B)**, COL4A3 **(C)**, and ITGBL1 **(D)** in LADC with and without EGFR mutation. Relative copy numbers normalized to GAPDH are plotted. mPAP+, tumors with the micropapillary element; mPAP-, tumors without the micropapillary element; EGFR (+), LADC with EGFR mutation; EGFR (-), LADC without EGFR mutation.

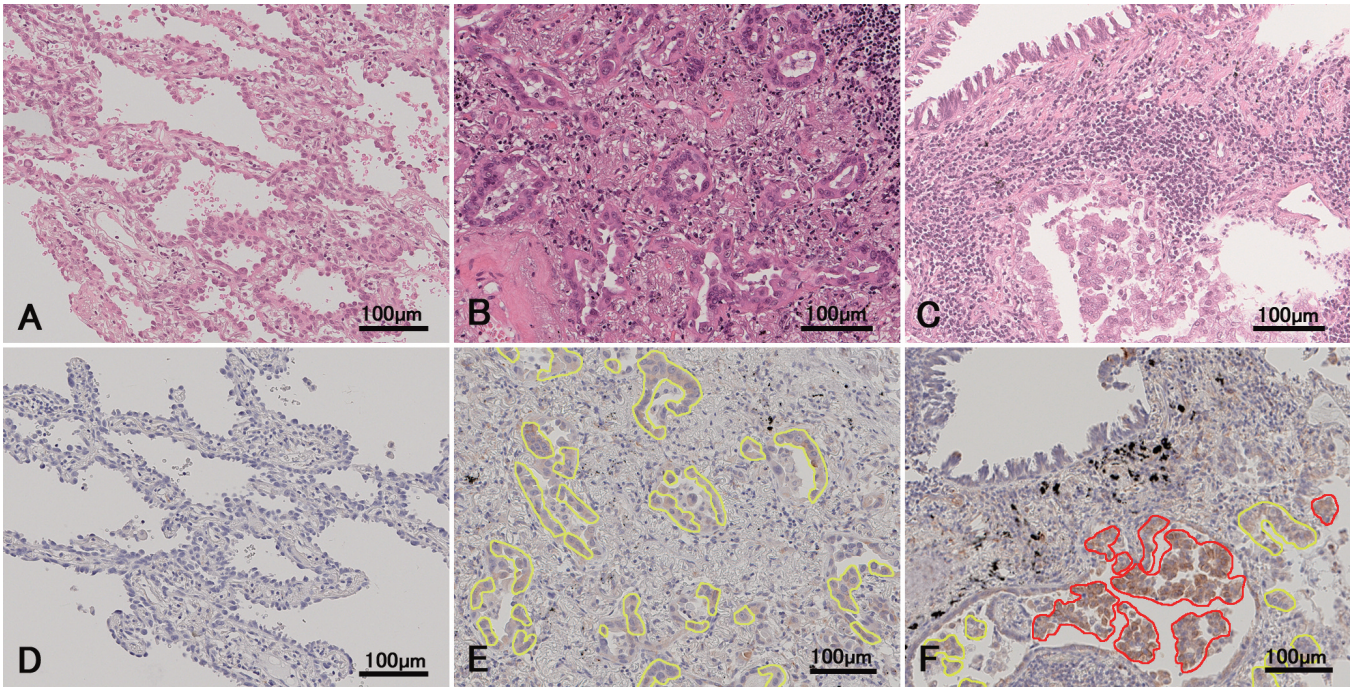

Fig. 5. Representative results of immunohistochemical staining of DYRK2 in different histological subtypes of *EGFR*-mutated LADC; lepidic **(A, D)**, acinar **(B, E)**, and micropapillary elements **(C, F)**. Tumor cells with no signal (intensity 0, not marked) **(D)**, weak signal (intensity 1, circumscribed with the yellow lines) **(E)**, and strong signal (intensity 2, circumscribed with the red lines) **(F)**. In the left panel **(D)**, no positive signal was detected throughout the tumor (score 0). In the center panel **(E)**, weak signals were detected in 80% of the tumor cells (score 80 = 1 × 80). In the right panel **(F)**, strong and weak signals were detected in 60% and 40% of the tumor cells, respectively (score 160 = 2 × 60 + 1 × 40). A, B, and C are hematoxylin and eosin-stained sections. D, E, and F are immunohistochemically stained for DYRK2. Scale bars: 100 μm.

Table 3. Clinicopathological characteristics of surgically resected lung adenocarcinomas.

	EGFR positive		*EGFR* negative	
	mPAP+ (n=58)	mPAP- (n=52)	ADC (n=20)	P value
Age (y/o)				0.732
Median (Range)	72 (49-88)	72 (48-88)	70.5 (52-90)	
Elder (>65)	45	38	13	
Younger (≤65)	27	34	7	
Gender				0.0001*
Female	37	41	5	
Male	21	11	15	
Smoking status				0.0008*
Non smoker	33	33	3	
Smoker	25	19	17	
Tumor size (mm)				0.6933
≤30 mm	45	43	17	
>30 mm	13	9	3	
Stage				0.0091
0, I	39	47	17	
II, III, IV	19	5	3	
Main histological subtype				<0.0001*
Lepidic*	21	41	11	
Acinar	22	6	2	
Papillary	11	4	2	
Micropapillary	2	0	0	
Solid	2	1	3	
Variants*	0	0	2	
mPAP average%				0.0043*
0-20%	48	0	5	
21-40%	9	0	1	
41-60%	0	0	0	
61-80%	1	0	0	
81-100%	0	0	0	
EGFR mutation type				0.0664
Major (exon19, exon21)	50	51	0	
Minor (exon18, exon20)	5	1	0	
Combined mutation	3			

mPAP+, tumor with micropapillary element; mPAP-, tumor without micropapillary element; ADC, adenocarcinoma irrespective subtype; EGFR, epidermal growth factor receptor; Stage, 8th Japanese classification of lung cancer; *Lepidic histological subtypes in this analysis include AIS and MIA; ** Variants, invasive mucinous adenocarcinoma and Enteric adenocarcinoma.

Table 4. Frequency of DYRK2 amplification between tumors with and without micropapillary element.

	Histological group		
	mPAP+ (n=33)	mPAP- (n=31)	P -value
DYRK2 amplification			0.0432
+	8	2	
-	25	29	

mPAP+, tumor with micropapillary element; mPAP-, tumor without micropapillary element; +, positive; -, negative; n, number of cases; P-values were calculated using Fisher's exact test.

Table 5. Association between DYRK2 amplification and p53 protein expression.

	DYRK2 amplification		
	Positive (n=10)	Negative (n=54)	p -value
p53			0.8007
+	2	9	
-	8	45	

+, positive; -, negative; n, number of cases; P-values were calculated using Fisher's exact test.

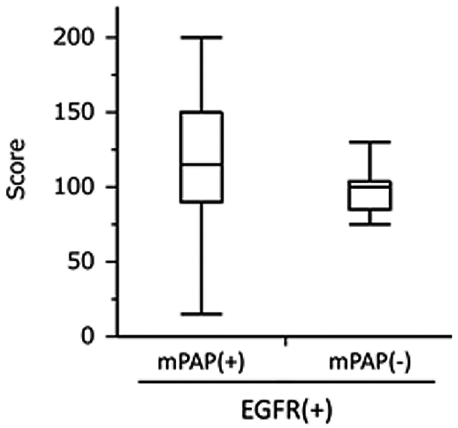

Fig. 6. Relationship between immunohistochemical scores of DYRK2 and histological subtypes in *EGFR*-mutated LADC. DYRK2 immunohistochemical scores are displayed as a box-and whiskers plot (median, thick line; 25th to 75th percentile, box; 10th to 90th percentile, whiskers). mPAP+, tumors with the micropapillary element; mPAP-, tumors without the micropapillary element.

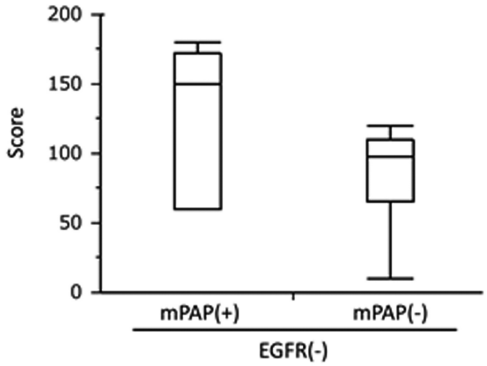

Fig. 7. Relationship between immunohistochemical scores of DYRK2 and histological subtypes in LADC without EGFR-mutation. DYRK2 immunohistochemical scores are displayed as a box-and whiskers plot (median, thick line; 25th to 75th percentile, box; 10th to 90th percentile, whiskers). mPAP+, tumors with the micropapillary element; mPAP-, tumors without the micropapillary element.

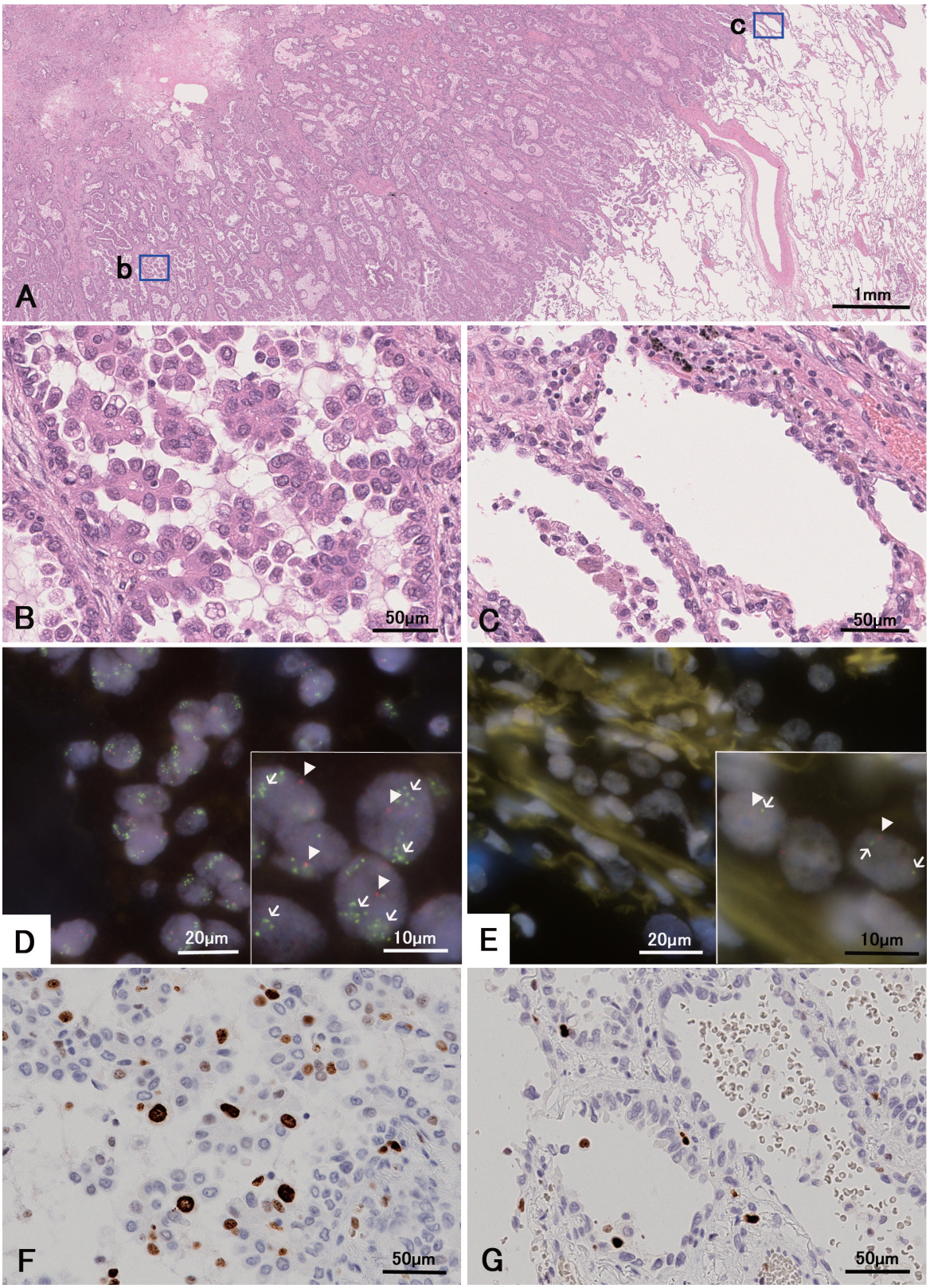

Fig. 8. Representative results of FISH analysis of DYRK2 and immunohistochemical staining for Ki-67 in *EGFR*-mutated LADC with the micropapillary element. Scanning view **(A)**, close-up view of square 'b' in panel A shows the micropapillary element **(B)**, and a close-up view of square 'c' in panel A shows the lepidic element **(C)**. The amplification of DYRK2 is observed in the micropapillary element **(D)**, but not in the lepidic element **(E)**; green signals show the DYRK2 gene locus (arrows) and orange signals the centromere of chromosome 12 (arrow heads). Ki-67-positive cells are more frequently observed in the micropapillary element **(F)** than in the lepidic element **(G)**. **A, B,** and **C** are the hematoxylin and eosin-stained sections. D and E are FISH analysis for DYRK2. F and G are immunohistochemically stained for Ki-67. Scale bars: A, 1 mm; B, C, F and G, 50 μm; D and E, 20 μm; inset in D and E, 10 μm.

element, although this was not statistically significant (Mann-Whitney U test, P=0.0983, Fig. 7).

Gene dosage of the DYRK2 locus

The 64 *EGFR*-mutated LADCs (33 mPAP-positive and 31 mPAP-negative tumors) were examined. In the tumors with the mPAP element, eight showed amplification of the *DYRK2* locus (24%, 8/33). Two of the tumors without the mPAP element showed DYRK2 amplification (6%, 2/31) (Table 4). Amplification was exclusively observed in the high-grade component consisting of mPAP and solid elements, but never in the low-grade component of the lepidic element (Fig. 8). The median FISH score was 3.2 in the high-grade component and 1.2 in the low-grade component among the ten tumors showing amplification (Fig. 9a). The difference was statistically significant (Wilcoxon signed-rank test, P<0.0001).

DYRK2 gene amplification and proliferation activity

In the ten tumors with *DYRK2* gene amplification, proliferation activities and Ki-67 labeling indexes were separately measured in tumor cells with the amplification and those without (Figs. 8, 9b). The Ki-67 labeling indexes were significantly higher in the high-grade component with amplification (Wilcoxon signed-rank test, p=0.0037).

DYRK2 gene amplification and disease recurrence

In the 64 *EGFR*-mutated LADC samples examined, a higher disease recurrence rate was observed in tumors with *DYRK2* gene amplification (30%, 3/10) than in those without the amplification (13%, 7/53).

DYRK2 gene amplification and p53 status

In the ten tumors with *DYRK2* gene amplification, two (20%) were positive for p53, whereas nine of the 54 tumors without *DYRK2* gene amplification (16%) were strongly positive for p53 (Table 5). Thus, there was no correlation between *DYRK2* gene amplification and p53 status.

Discussion

The present study aimed to elucidate the molecular mechanisms producing the mPAP element of *EGFR*-mutated LADC. Herein, through comprehensive mRNA expression analysis of the mPAP element, we identified DYRK2. Using immunohistochemical analysis, we demonstrated the frequent upregulation of DYRK2 expression in the mPAP element, which appeared to be caused by gene amplification.

Previous studies demonstrated that DYRK2 was overexpressed in LADC and esophageal cancer, suggesting that its overexpression is associated with tumor development and/or progression (Miller et al., 2003). Our results also revealed a higher disease recurrence rate in cases with DYRK2 amplification. These results support the notion that upregulation of DYRK2 expression promotes the progression of LADC. In contrast, previous studies have reported that the downregulation of DYRK2 expression is associated with

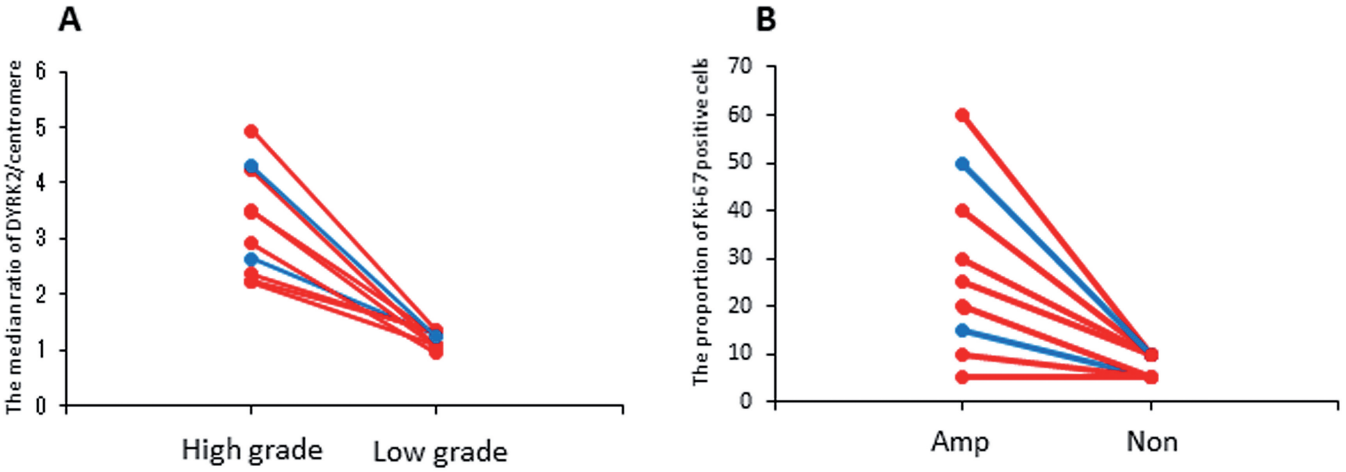

Fig. 9. DYRK2 FISH scores in high-grade and low-grade components of *EGFR*-mutated LADC. Ten tumors with the amplification of DYRK2 were examined, and the separately calculated high-grade and low-grade component FISH scores are plotted. Median FISH score is 3.2 in the high-grade component and 1.2 in the low-grade component (Wilcoxon signed-rank test, P < 0.0001) **(A)**. Proliferation activities, measured by the proportion of Ki-67 labeling index, were separately obtained for tumor cells with and without DYRK2 amplification. The Ki-67 labeling index was significantly higher in the DYRK2-amplified cells (Amp) than in the cells without DYRK2 amplification (Non) (Wilcoxon signed-rank test, p = 0.0037) **(B)**. In both graphs, red dots/lines indicate tumors with the micropapillary element, and blue dots/lines indicate those without the micropapillary element.

a poorer outcome in liver cancer, colorectal cancer, and ovarian serous adenocarcinoma (Yamaguchi et al., 2015; Zhang et al., 2016). Moreover, in lung cancer, high levels of DYRK2 expression have been reported to be associated with favorable postoperative survival (Yamashita et al., 2009a) and response to chemotherapy (Yamashita et al., 2009b). These findings are inconsistent with our current results. However, in these previous studies, the relationship between DYRK2 levels and disease outcome was not analyzed specifically among the different histological subtypes. Thus, DYRK2 appears to play diverse roles in carcinogenesis, and the clinical outcome may depend on the type of cancer. Therefore, further studies on the biological functions of DYRK2 in different cancer types and their histological subtypes are warranted.

DYRK2 is a member of the dual-specificity tyrosine-(Y)-phosphorylation-regulated kinase family, which plays important roles in cell growth, differentiation, and survival by regulating the activities of some tumor suppressors and oncogenes, including p53, c-Jun, c-Myc, hPXR, and SIAH2 (Maddika and Chen, 2009; Perez et al., 2012). p53, the most common tumor suppressor, has been shown to play a crucial role in the progression of LADC (Hollstein et al., 1991; Robles and Harris, 2010). DYRK2 directly phosphorylates p53 to negatively regulate its activity, which affects the induction of apoptosis, consequently promoting tumor progression (Taira et al., 2007; Nihira and Yoshida, 2015). Thus, we hypothesized that a gain of function in DYRK2 and loss of function in p53 may be mutually exclusive events because each may exert the same effect on tumor progression. To evaluate this hypothesis, we immunohistochemically analyzed the potential relationship between *DYRK2* amplification and p53 accumulation (resulting from mutation) in *EGFR*-mutated LADCs. However, no correlation was observed between *DYRK2* amplification and p53 accumulation. Therefore, DYRK2 likely regulates another pathway.

However, even in the LADCs without EGFR mutation, tumors with the mPAP element showed slightly higher levels of DYRK2 expression. Thus, DYRK2 may participate in producing the mPAP elements irrespective of EFGR mutation status.

In conclusion, we identified DYRK2 as a key molecule associated with the mPAP element that may promote the progression of *EGFR*-mutated LADC. To the best of our knowledge, this is the first study to show the potential involvement of *DYRK2* amplification in producing the mPAP element in LADC.

Acknowledgements. We thank Emi Honda, Misaki Sugiyama, and Motoki Sekiya (Division of Pathology, Kanagawa Prefectural Cardiovascular, and Respiratory Center Hospital) for their technical assistance. This work was supported by the Japanese Ministry of Education, Culture, Sports, and Science (Tokyo, Japan).

Conflicts of interest. The authors declare that they have no conflicts of interest.

References

Gainor J.F. and Shaw A.T. (2013). Novel targets in non-small cell lung cancer: Ros1 and ret fusions. Oncologist 18, 865-875.

Gainor J.F., Varghese A.M., Ou S.H., Kabraji S., Awad M.M., Katayama R., Pawlak A., Mino-Kenudson M., Yeap B.Y., Riely G.J., Iafrate A.J., Arcila M.E., Ladanyi M., Engelman J.A., Dias-Santagata D. and Shaw A.T. (2013). Alk rearrangements are mutually exclusive with mutations in egfr or kras: An analysis of 1,683 patients with non-small cell lung cancer. Clin. Cancer Res. 19, 4273-4281.

Goto K., Satouchi M., Ishii G., Nishio K., Hagiwara K., Mitsudomi T., Whiteley J., Donald E., McCormack R. and Todo T. (2012). An evaluation study of egfr mutation tests utilized for non-small-cell lung cancer in the diagnostic setting. Ann. Oncol. 23, 2914-2919.

Guo C.C., Dadhania V., Zhang L., Majewski T., Bondaruk J., Sykulski M., Wronowska W., Gambin A., Wang Y., Zhang S., Fuentes-Mattei E., Kamat A.M., Dinney C., Siefker-Radtke A., Choi W., Baggerly K.A., McConkey D., Weinstein J.N. and Czerniak B. (2016). Gene expression profile of the clinically aggressive micropapillary variant of bladder cancer. Eur. Urol. 70, 611-620.

Hollstein M., Sidransky D., Vogelstein B. and Harris C.C. (1991). P53 mutations in human cancers. Science 253, 49-53.

Kadota K., Villena-Vargas J., Yoshizawa A., Motoi N., Sima C.S., Riely G.J., Rusch V.W., Adusumilli P.S. and Travis W.D. (2014). Prognostic significance of adenocarcinoma *in situ*, minimally invasive adenocarcinoma and nonmucinous lepidic predominant invasive adenocarcinoma of the lung in patients with stage I disease. Am. J. Surg. Pathol. 38, 448-460.

Kanomata N., Kurebayashi J., Koike Y., Yamaguchi R. and Moriya T. (2019). CD1d- and PJA2-related immune microenvironment differs between invasive breast carcinomas with and without a micropapillary feature. BMC Cancer 19, 76.

Kimura H., Kasahara K., Kawaishi M., Kunitoh H., Tamura T., Holloway B. and Nishio K. (2006). Detection of epidermal growth factor receptor mutations in serum as a predictor of the response to gefitinib in patients with non-small-cell lung cancer. Clin. Cancer Res. 12, 3915-3921.

Kosaka T., Yatabe Y., Endoh H., Kuwano H., Takahashi T. and Mitsudomi T. (2004). Mutations of the epidermal growth factor receptor gene in lung cancer: Biological and clinical implications. Cancer Res. 64, 8919-8923.

Lynch T.J., Bell D.W., Sordella R., Gurubhagavatula S., Okimoto R.A., Brannigan B.W., Harris P.L., Haserlat S.M., Supko J.G., Haluska F.G., Louis D.N., Christiani D.C., Settleman J. and Haber D.A. (2004). Activating mutations in the epidermal growth factor receptor underlying responsiveness of non-small-cell lung cancer to gefitinib. N. Engl. J. Med. 350, 2129-2139.

Maddika S. and Chen J. (2009). Protein kinase DYRK2 is a scaffold that facilitates assembly of an E3 ligase. Nat. Cell Biol. 11, 409-419.

Matsumura M., Okudela K., Kojima Y., Umeda S., Tateishi Y., Sekine A., Arai H., Woo T., Tajiri M. and Ohashi K. (2016). A histopathological feature of *egfr*-mutated lung adenocarcinomas with highly malignant potential - an implication of micropapillary element. PLoS One 11, e0166795.

Miller C.T., Aggarwal S., Lin T.K., Dagenais S.L., Contreras J.I., Orringer M.B., Glover T.W., Beer D.G. and Lin L. (2003). Amplification and overexpression of the dual-specificity tyrosine-(y)-phosphorylation regulated kinase 2 (DYRK2) gene in esophageal and lung adenocarcinomas. Cancer Res. 63, 4136-4143.

Nihira N.T. and Yoshida K. (2015). Engagement of DYRK2 in proper control for cell division. Cell Cycle. 14, 802-807.

Okudela K., Woo T., Yazawa T., Ogawa N., Tajiri M., Masuda M. and Kitamura H. (2009). Significant association between *egfr*-mutated lung adenocarcinoma and past illness from gastric cancer or uterine myoma: Its implication in carcinogenesis. Lung Cancer 66, 287-291.

Okudela K., Woo T., Mitsui H., Yazawa T., Shimoyamada H., Tajiri M., Ogawa N., Masuda M. and Kitamura H. (2010). Morphometric profiling of lung cancers-its association with clinicopathologic, biologic, and molecular genetic features. Am. J. Surg. Pathol. 34, 243-255.

Ou S.H. (2011). Crizotinib: A novel and first-in-class multitargeted tyrosine kinase inhibitor for the treatment of anaplastic lymphoma kinase rearranged non-small cell lung cancer and beyond. Drug. Des. Devel. Ther. 5, 471-485.

Paez J.G., Janne P.A., Lee J.C., Tracy S., Greulich H., Gabriel S., Herman P., Kaye F.J., Lindeman N., Boggon T.J., Naoki K., Sasaki H., Fujii Y., Eck M.J., Sellers W.R., Johnson B.E. and Meyerson M. (2004). EGFR mutations in lung cancer: Correlation with clinical response to gefitinib therapy. Science 304, 1497-1500.

Patankar M., Väyrynen S., Tuomisto A., Mäkinen M., Eskelinen S. and Karttunen T.J. (2018). Micropapillary structures in colorectal cancer: An anoikis-resistant subpopulation. Anticancer Res. 38, 2915-2921.

Perez M., Garcia-Limones C., Zapico I., Marina A., Schmitz M.L., Munoz E. and Calzado M.A. (2012). Mutual regulation between SIAH2 and DYRK2 controls hypoxic and genotoxic signaling pathways. J. Mol. Cell Biol. 4, 316-330.

Robles A.I. and Harris C.C. (2010). Clinical outcomes and correlates of TP53 mutations and cancer. Cold Spring Harb. Perspect. Biol. 2, a001016.

Soda M., Choi Y.L., Enomoto M., Takada S., Yamashita Y., Ishikawa S., Fujiwara S., Watanabe H., Kurashina K., Hatanaka H., Bando M., Ohno S., Ishikawa Y., Aburatani H., Niki T., Sohara Y., Sugiyama Y. and Mano H. (2007). Identification of the transforming EML4-ALK fusion gene in non-small-cell lung cancer. Nature 448, 561-566.

Taira N., Nihira K., Yamaguchi T., Miki Y. and Yoshida K. (2007). DYRK2 is targeted to the nucleus and controls p53 via ser46 phosphorylation in the apoptotic response to DNA damage. Mol. Cell. 25, 725-738.

Takeuchi K., Soda M., Togashi Y., Suzuki R., Sakata S., Hatano S., Asaka R., Hamanaka W., Ninomiya H., Uehara H., Lim Choi Y., Satoh Y., Okumura S., Nakagawa K., Mano H. and Ishikawa Y. (2012). RET, ROS1 and ALK fusions in lung cancer. Nat. Med. 18, 378-381.

Travis W.D., Noguchi M., Yatabe Y., Brambilla E., Nicholson A.G., Aisner S.C. and Austin J.H.M. (2015). Adenocarcinoma. In: Who classification of tumours of the lung, pleura, thymus and heart, Travis W.D., Brambilla E., Burke A.P., Marx A. and Micholson A.G. (eds). IARC Press. Lyon.

Villa C., Cagle P.T., Johnson M., Patel J.D., Yeldandi A.V., Raj R., DeCamp M.M. and Raparia K. (2014). Correlation of EGFR mutation status with predominant histologic subtype of adenocarcinoma according to the new lung adenocarcinoma classification of the international association for the study of lung cancer/american thoracic society/european respiratory society. Arch. Pathol. Lab. Med. 138, 1353-1357.

Warth A., Muley T., Meister M., Stenzinger A., Thomas M., Schirmacher P., Schnabel P.A., Budczies J., Hoffmann H. and Weichert W. (2012). The novel histologic international association for the study of lung cancer/american thoracic society/european respiratory society classification system of lung adenocarcinoma is a stage-independent predictor of survival. J. Clin. Oncol. 30, 1438-1446.

Yamaguchi N., Mimoto R., Yanaihara N., Imawari Y., Hirooka S., Okamoto A. and Yoshida K. (2015). DYRK2 regulates epithelial-mesenchymal-transition and chemosensitivity through snail degradation in ovarian serous adenocarcinoma. Tumour Biol. 36, 5913-5923.

Yamashita S., Chujo M., Tokuishi K., Anami K., Miyawaki M., Yamamoto S. and Kawahara K. (2009a). Expression of dual-specificity tyrosine-(y)-phosphorylation-regulated kinase 2 (DYRK2) can be a favorable prognostic marker in pulmonary adenocarcinoma. J. Thorac. Cardiovasc. Surg. 138, 1303-1308.

Yamashita S., Chujo M., Moroga T., Anami K., Tokuishi K., Miyawaki M., Kawano Y., Takeno S., Yamamoto S. and Kawahara K. (2009b). Dyrk2 expression may be a predictive marker for chemotherapy in non-small cell lung cancer. Anticancer Res. 29, 2753-2757.

Zhang J., Sun J., Zhang Z., Liang X., Luo Y., Wu S. and Liang Z. (2018). Protein overexpression and gene amplification of cellular mesenchymal-epithelial transition factor is associated with poor prognosis in micropapillary-predominant subtype pulmonary adenocarcinoma. Hum. Pathol. 72, 59-65.

Zhang X., Xu P., Ni W., Fan H., Xu J., Chen Y., Huang W., Lu S., Liang L., Liu J., Chen B. and Shi W. (2016). Downregulated DYRK2 expression is associated with poor prognosis and oxaliplatin resistance in hepatocellular carcinoma. Pathol. Res. Pract. 212, 162-170.

Accepted December 22, 2020